5432 *Inorg. Chem.* **2010**, *49*, 5432–5443
DOI: 10.1021/ic902443e

Inorganic Chemistry
Article

Luminescent Dendritic Cyclometalated Iridium(III) Polypyridine Complexes: Synthesis, Emission Behavior, and Biological Properties

Kenneth Yin Zhang, Hua-Wei Liu, Tommy Tsz-Him Fong, Xian-Guang Chen, and Kenneth Kam-Wing Lo*

Department of Biology and Chemistry, City University of Hong Kong, Tat Chee Avenue, Kowloon, Hong Kong, People's Republic of China

Received December 9, 2009

Luminescent dendritic cyclometalated iridium(III) polypyridine complexes $[\{Ir(N^\wedge C)_2\}_n(bpy\text{-}n)](PF_6)_n$ (HN^C = 2-phenylpyridine, Hppy, n = 8 (**ppy-8**), 4 (**ppy-4**), 3 (**ppy-3**); HN^C = 2-phenylquinoline, Hpq, n = 8 (**pq-8**), 4 (**pq-4**), 3 (**pq-3**)) have been designed and synthesized. The properties of these dendrimers have been compared to those of their monomeric counterparts $[Ir(N^\wedge C)_2(bpy\text{-}1)](PF_6)$ (HN^C = Hppy (**ppy-1**), Hpq (**pq-1**)). Cyclic voltammetric studies revealed that the iridium(IV/III) oxidation and bpy-based reduction occurred at about +1.24 to +1.29 V and −1.21 to −1.27 V versus SCE, respectively, for all the complexes. The molar absorptivity of the dendritic iridium(III) complexes is approximately proportional to the number of $[Ir(N^\wedge C)_2(N^\wedge N)]$ moieties in one complex molecule. However, the emission lifetimes and quantum yields are relatively independent of the number of $[Ir(N^\wedge C)_2(N^\wedge N)]$ units, suggesting negligible electronic communications between these units. Upon photoexcitation, the complexes displayed triplet metal-to-ligand charge-transfer (^{3}MLCT) ($d\pi(Ir) \rightarrow \pi^*(bpy\text{-}n)$) emission. The interaction of these complexes with plasmid DNA has been investigated by agarose gel retardation assays. The results showed that the dendritic iridium(III) complexes, unlike their monomeric counterparts, bound to the plasmid, and the interaction was electrostatic in nature. The lipophilicity of all the complexes has been determined by reversed-phase high-performance liquid chromatography (HPLC). Additionally, the cellular uptake of the complexes by the human cervix epithelioid carcinoma (HeLa) cell line has been examined by inductively coupled plasma mass spectrometry (ICP-MS), laser-scanning confocal microscopy, and flow cytometry. Upon internalization, all the complexes were localized in the perinuclear region, forming very sharp luminescent rings surrounding the nuclei. Interestingly, in addition to these rings, HeLa cells treated with the dendritic iridium(III) complexes showed specific labeled compartments, which have been identified to be the Golgi apparatus. Furthermore, the cytotoxicity of these iridium(III) complexes has been evaluated by the 3-(4,5-dimethyl-2-thiazolyl)-2,5-diphenyltetrazolium bromide (MTT) assay.

Introduction

The role of dendrimers in biomedical applications has attracted increasing interest.[1−4] They have been used as transfection agents for gene therapy (GT),[5,6] contrast agents for magnetic resonance imaging (MRI),[7−9] reagents in boron neutron capture therapy (BNCT) for cancer treatment,[5,10] and carriers for selective drug delivery.[4,11] Their hyperbranched structures usually lead to a desired motif in a multivalent fashion, giving synergistic enhancement of a particular function. To trail the localization and distribution of these dendrimers in live cells and organisms, various labels such as organic fluorophores have been linked to the termini to give detectable signals.[3,12−14]

Luminescent transition metal complexes have been introduced to dendritic systems because of their favorable properties

*To whom correspondence should be addressed. E-mail: bhkenlo@cityu.edu.hk. Phone: (852) 2788 7231. Fax: (852) 2788 7406.

(1) Caminade, A.-M.; Turrin, C.-O.; Majoral, J.-P. *Chem.—Eur. J.* **2008**, *14*, 7422–7432.
(2) Astruc, D.; Ornelas, C.; Ruiz, J. *Acc. Chem. Res.* **2008**, *41*, 841–856.
(3) Ortega, P.; Serramía, M. J.; Samaniego, R.; de la Mata, F. J.; Gomez, R.; Muñoz-Fernandez, M. A. *Org. Biomol. Chem.* **2009**, *7*, 3079–3085.
(4) Shcharbin, D. G.; Klajnert, B.; Bryszewska, M. *Biochemistry (Moscow)* **2009**, *74*, 1314–1326.
(5) Majoros, I. J.; Williams, C. R.; J. R. Baker, J. R., Jr. *Curr. Top. Med. Chem.* **2008**, *8*, 1165–1179.
(6) Mei, M.; Ren, Y.; Zhou, X.; Yuan, X.-B.; Li, F.; Jiang, L.-H.; Kang, C.-S.; Yao, Z. *J. Appl. Polym. Sci.* **2009**, *114*, 3760–3766.
(7) Talanov, V. S.; Regino, C. A. S.; Kobayashi, H.; Bernardo, M.; Choyke, P. L.; Brechbiel, M. W. *Nano Lett.* **2006**, *6*, 1459–1463.
(8) Shi, X.; Wang, S. H.; Swanson, S. D.; Ge, S.; Cao, Z.; Van Antwerp, M. E.; Landmark, K. J.; Baker, J. R., Jr. *Adv. Mater.* **2008**, *20*, 1671–1678.
(9) Ali, M. M.; Woods, M.; Caravan, P.; L. Opina, A. C.; Spiller, M.; Fettinger, J. C.; Sherry, A. D. *Chem.—Eur. J.* **2008**, *14*, 7250–7258.
(10) Barth, R. F.; Adams, D. M.; Soloway, A. H.; Alam, F.; Darbyt, M. V. *Bioconjugate Chem.* **1994**, *5*, 58–66.
(11) Kurtoglu, Y. E.; Navath, R. S.; Wang, B.; Kannan, S.; Romero, R.; Kannan, R. M. *Biomaterials* **2009**, *30*, 2112–2121.
(12) Khandare, J.; Kolhe, P.; Pillai, O.; Kannan, S.; Lieh-Lai, M.; Kannan, R. M. *Bioconjugate Chem.* **2005**, *16*, 330–337.
(13) Fuchs, S.; Otto, H.; Jehle, S.; Henkleinc, P.; Schlüter, A. D. *Chem. Commun.* **2005**, 1830–1832.
(14) Saovapakhiran, A.; D'Emanuele, A.; Attwood, D.; Penny, J. *Bioconjugate Chem.* **2009**, *20*, 693–701.

Published on Web 05/21/2010

such as high photostability, long emission lifetimes, and large Stokes' shifts.[15−24] In this context, luminescent dendrimers with an iridium(III) complex core have been designed in the development of organic light-emitting diodes[20,21] and electrophosphorescent light-emitting devices.[22,23] Despite these studies, the possibility of applying luminescent dendrimers containing iridium(III) polypyridine complexes in biological work has not been explored.[24] In view of the interesting emissive behavior of iridium(III) polypyridine complexes,[25−43] and our recent work on the mononuclear complexes of this type in biological studies,[43] we believe that it will be interesting to investigate the potential applications of polynuclear complexes or dendrimers modified with luminescent cyclometalated iridium(III) polypyridine complexes as new probes for biological molecules and live cells. The objectives of this work are based on the following considerations: (1) an increasing number of luminescent units in a macromolecular probe may alter its photophysical properties which could offer new biological sensing possibilities; (2) an increase of formal charge of a dendrimer because of the addition of cationic $[Ir(N^{\wedge}C)_2(N^{\wedge}N)]^+$ units is expected to change the biological behavior of the resultant adduct; (3) while a change of the ligand and hence the lipophilicity of the mononuclear complex $[Ir(N^{\wedge}C)_2(N^{\wedge}N)]^+$ has been found to significantly perturb its biomolecular binding, cellular uptake, and cytotoxic properties,[43a,e,g,h,j−l] it will be interesting to investigate whether these effects will still be observed when the complexes are linked together by a dendritic skeleton; and (4) most importantly, while the biological and cellular uptake properties of mononuclear cyclometalated iridium(III) polypyridine complexes modified with various biologically relevant

(15) Zhu, L.; Magde, D.; Whitesell, J. K.; Fox, M. A. *Inorg. Chem.* **2009**, *48*, 1811–1818.
(16) McClenaghan, N. D.; Passalacqua, R.; Loiseau, F.; Campagna, S.; Verheyde, B.; Hameurlaine, A.; Dehaen, W. *J. Am. Chem. Soc.* **2003**, *125*, 5356–5365.
(17) Zhou, X.; Tyson, D. S.; Castellano, F. N. *Angew. Chem., Int. Ed.* **2000**, *39*, 4301–4305.
(18) (a) Issberner, J.; Vögtle, F.; De Cola, L.; Balzani, V. *Chem.—Eur. J.* **1997**, *3*, 706–712. (b) Plevoets, M.; Vögtle, F.; De Cola, L.; Balzani, V. *New J. Chem.* **1999**, 63–69. (c) Vögtle, F.; Plevoets, M.; Nieger, M.; Azzellini, G. C.; Credi, A.; De Cola, L.; De Marchis, V.; Venturi, M.; Balzani, V. *J. Am. Chem. Soc.* **1999**, *121*, 6290–6298. (d) Staffilani, M.; Höss, E.; Giesen, U.; Schneider, E.; Hartl, F.; Josel, H.-P.; De Cola, L. *Inorg. Chem.* **2003**, *52*, 7789–7798. (e) Dirksen, A.; De Cola, L. *C. R. Chim.* **2003**, *6*, 873–882. (f) Hahn, W.; Vögtle, F.; De Paoli, G.; Staffilani, M.; De Cola, M. *Eur. J. Inorg. Chem.* **2009**, 2639–2646.
(19) Li, Y.; Rizzo, A.; Salerno, M.; Mazzeo, M.; Huo, C.; Wang, Y.; Li, K.; Cingolani, R.; Gigli, G. *Appl. Phys. Lett.* **2006**, *89*, 061125.
(20) (a) Zhou, G.; Wong, W.-Y.; Yao, B.; Xie, Z.; Wang, L. *Angew. Chem., Int. Ed.* **2007**, *46*, 1149–1151. (b) Qin, T.; Ding, J.; Wang, L.; Baumgarten, M.; Zhou, G.; Müllen, K. *J. Am. Chem. Soc.* **2009**, *131*, 14329–14336.
(21) Lo, S.-C.; Harding, R. E.; Shipley, C. P.; Stevenson, S. G.; Burn, P. L.; Samuel, I. D. W. *J. Am. Chem. Soc.* **2009**, *131*, 16681–16688.
(22) Ding, J.; Wang, B.; Yue, Z.; Yao, B.; Xie, Z.; Cheng, Y.; Wang, L.; Jing, X.; Wang, F. *Angew. Chem., Int. Ed.* **2009**, *48*, 6664–6666.
(23) Li, X.; Chen, Z.; Zhao, Q.; Shen, L.; Li, F.; Yi, T.; Cao, Y.; Huang, C. *Inorg. Chem.* **2007**, *46*, 5518–5527.
(24) The biological properties of dendrimers containing inorganic and organometallic complexes have been investigated. See, for example: (a) Malik, N.; Evagorou, E. G.; Duncan, R. *Anti-Cancer Drugs* **1999**, *10*, 767–776. (b) Jansen, B. A. J.; van des Zwan, J.; Reedijk, J.; den Dulk, H.; Brouwer, J. *Eur. J. Inorg. Chem.* **1999**, 1429–1433. (c) Heldt, J.-M.; Fischer-Durand, N.; Salmain, M.; Vessières, A.; Jaouen, G. *J. Organomet. Chem.* **2004**, *689*, 4775–4782. (d) Kapp, T.; Dullin, A.; Gust, R. *J. Med. Chem.* **2006**, *49*, 1182–1190. (e) Govender, P.; Antonels, N. C.; Mattsson, J.; Renfrew, A. K.; Dyson, P. J.; Moss, J. R.; Therrien, B.; Smith, G. S. *J. Organomet. Chem.* **2009**, *694*, 3470–3476.
(25) (a) Sprouse, S.; King, K. A.; Spellane, P. J.; Watts, R. J. *J. Am. Chem. Soc.* **1984**, *106*, 6647–6653. (b) King, K. A.; Watts, R. J. *J. Am. Chem. Soc.* **1987**, *109*, 1589–1590.
(26) (a) Didier, P.; Ortmans, I.; Kirsch-De Mesmaeker, A.; Watts, R. J. *Inorg. Chem.* **1993**, *32*, 5239–5245. (b) Ortmans, I.; Didier, P.; Kirsch-De Mesmaeker, A. *Inorg. Chem.* **1995**, *34*, 3695–3704.
(27) (a) Holder, E.; Marin, V.; Kozodaev, D.; Meier, M. A. R.; Lohmeijer, B. G. G.; Schubert, U. S. *Macromol. Chem. Phys.* **2005**, *206*, 989–997. (b) Marin, V.; Holder, E.; Hoogenboom, R.; Tekin, E.; Schubert, U. S. *Dalton Trans.* **2006**, 1636–1644.
(28) (a) Dixon, I. M.; Collin, J.-P.; Sauvage, J.-P.; Flamigni, L.; Encinas, S.; Barigelletti, F. *Chem. Soc. Rev.* **2000**, *29*, 385–391. (b) Auffrant, A.; Barbieri, A.; Barigelletti, F.; Lacour, J.; Mobian, P.; Collin, J.-P.; Sauvage, J.-P.; Ventura, B. *Inorg. Chem.* **2007**, *46*, 6911–6919.
(29) (a) Neve., F.; La Deda, M.; Puntoriero, F.; Campagna, S. *Inorg. Chim. Acta* **2006**, *359*, 1666–1672. (b) Natstasi, F.; Puntoriero, F.; Campagna, S.; Schergna, S.; Maggini, M.; Cardinali, F.; Delavaux-Nicot, B.; Nierengarten, J.-F. *Chem. Commun.* **2007**, 3556–3558.
(30) (a) Hirani, B.; Li, J.; Djurovich, P. I.; Yousufuddin, M.; Oxgaard, J.; Persson, P.; Wilson, S. R.; Bau, R.; Goddard, W. A., III; Thompson, M. E. *Inorg. Chem.* **2007**, *46*, 3865–3875. (b) Finkenzeller, W. J.; Hofbeck, T.; Thompson, M. E.; Yersin, H. *Inorg. Chem.* **2007**, *46*, 5076–5083.
(31) (a) Di Censo, D.; Fantacci, S.; De Angelis, F.; Klein, C.; Evans, N.; Kalyanasundaram, K.; Bolink, H. J.; Grätzel, M.; Nazeeruddin, M. K. *Inorg. Chem.* **2008**, *47*, 980–989. (b) Baranoff, E.; Suàrez, S.; Bugnon, P.; Barolo, C.; Buscaino, R.; Scopelliti, R.; Zuppiroli, L.; Graetzel, M.; Nazeeruddin, Md. K. *Inorg. Chem.* **2008**, *47*, 6575–6577.
(32) (a) Williams, J. A. G.; Wilkinson, A. J.; Whittle, V. L. *Dalton Trans.* **2008**, 2081–2099. (b) Whittle, V. L.; Williams, J. A. G. *Inorg. Chem.* **2008**, *47*, 6596–6607.
(33) (a) Polson, M.; Fracasso, S.; Bertolasi, V.; Ravaglia, M.; Scandola, F. *Inorg. Chem.* **2004**, *43*, 1950–1956. (b) Polson, M.; Ravaglia, M.; Fracasso, S.; Garavelli, M.; Scandola, F. *Inorg. Chem.* **2005**, *44*, 1282–1289.
(34) (a) Guerrero-Martínez, A.; Vida, Y.; Domínguez-Gutiérrez, D.; Albuquerque, R. Q.; De Cola, L. *Inorg. Chem.* **2008**, *47*, 9131–9133. (b) Stagni, S.; Colella, S.; Palazzi, A.; Valenti, G.; Zacchini, S.; Paolucci, F.; Marcaccio, M.; Albuquerque, R. Q.; De Cola, L. *Inorg. Chem.* **2008**, *47*, 10509–10521.
(35) (a) Obara, S.; Itabashi, M.; Okuda, F.; Tamaki, S.; Tanabe, Y.; Ishii, Y.; Nozaki, K.; Haga, M. *Inorg. Chem.* **2006**, *45*, 8907–8921. (b) Yang, L.; Okuda, F.; Kobayashi, K.; Nozaki, K.; Tanabe, Y.; Ishii, Y.; Haga, M. *Inorg. Chem.* **2008**, *47*, 7154–7165.
(36) (a) Zysman-Colman, E.; Slinker, J. D.; Parker, J. B.; Malliaras, G. G.; Bernhard, S. *Chem. Mater.* **2008**, *20*, 388–396. (b) Coughlin, F. J.; Westrol, M. S.; Oyler, K. D.; Byrne, N.; Kraml, C.; Zysman-Colman, E.; Lowry, M. S.; Bernhard, S. *Inorg. Chem.* **2008**, *47*, 2039–2048.
(37) (a) Yang, C.-H.; Cheng, Y.-M.; Chi, Y.; Hsu, C.-J.; Fang, F.-C.; Wong, K.-T.; Chou, P.-T.; Chang, C.-H.; Tsai, M.-H.; Wu, C. C. *Angew. Chem., Int. Ed.* **2007**, *46*, 2418–2421. (b) Chang, C.-F.; Cheng, Y.-M.; Chi, Y.; Chiu, Y.-C.; Lin, C.-C.; Lee, G.-H.; Chou, P.-T.; Chen, C.-C.; Chang, C.-H.; Wu, C. C. *Angew. Chem., Int. Ed.* **2008**, *47*, 4542–4545.
(38) (a) Zhao, Q.; Li, L.; Li, F.; Yu, M.; Liu, Z.; Yi, T.; Huang, C. *Chem. Commun.* **2008**, 685–687. (b) Yu, M.; Zhao, Q.; Shi, L.; Li, F.; Zhou, Z.; Yang, H.; Yi, T.; Huang, C. *Chem. Commun.* **2008**, 2115–2117.
(39) Dragonetti, C.; Falciola, L.; Mussini, P.; Righetto, S.; Roberto, D.; Ugo, R.; Valore, A.; De Angelis, F.; Fantacci, S.; Sgamellotti, A.; Ramon, M.; Muccini, M. *Inorg. Chem.* **2007**, *46*, 8533–8547.
(40) Zeng, X.; Tavasli, M.; Perepichka, I. F.; Batsanov, A. S.; Bryce, M. R.; Chiang, C.-J.; Rothe, C.; Monkman, A. P. *Chem.—Eur. J.* **2008**, *14*, 933–943.
(41) Freys, J. C.; Bernardinellib, G.; Wenger, O. S. *Chem. Commun.* **2008**, 4267–4269.
(42) Kwon, T.-H.; Kwon, J.; Hong, J.-I. *J. Am. Chem. Soc.* **2008**, *130*, 3726–3727.
(43) (a) Lo, K. K.-W.; Li, C.-K.; Lau, J. S.-Y. *Organometallics* **2005**, *24*, 4594–4601. (b) Lo, K. K.-W.; Hui, W.-K.; Chung, C.-K.; Tsang, K. H.-K.; Ng, D. C.-M.; Zhu, N.; Cheung, K.-K. *Coord. Chem. Rev.* **2005**, *249*, 1434–1450. (c) Lo, K. K.-W.; Chung, C.-K.; Zhu, N. *Chem.—Eur. J.* **2006**, *12*, 1500–1512. (d) Lo, K. K.-W.; Tsang, K. H.-K.; Sze, K.-S.; Chung, C.-K.; Lee, T. K.-M.; Zhang, K. Y.; Hui, W.-K.; Li, C.-K.; Lau, J. S.-Y.; Ng, D. C.-M.; Zhu, N. *Coord. Chem. Rev.* **2007**, *251*, 2292–2310. (e) Lo, K. K.-W.; Zhang, K. Y.; Chung, C.-K.; Kwok, K. Y. *Chem.—Eur. J.* **2007**, *13*, 7110–7130. (f) Lo, K. K.-W.; Zhang, K. Y.; Leung, S.-K.; Tang, M.-C. *Angew. Chem., Int. Ed.* **2008**, *47*, 2213–2216. (g) Lo, K. K.-W.; Lee, P.-K.; Lau, J. S.-Y. *Organometallics* **2008**, *27*, 2998–3006. (h) Lau, J. S.-Y.; Lee, P.-K.; Tsang, K. H.-K.; Ng, C. H.-C.; Lam, Y.-W.; Cheng, S.-H.; Lo, K. K.-W. *Inorg. Chem.* **2009**, *48*, 708–718. (i) Zhang, K. Y.; Lo, K. K.-W. *Inorg. Chem.* **2009**, *48*, 6011–6025. (j) Zhang, K. Y.; Li, S. P.-Y.; Zhu, N.; Or, I. W.-S.; Cheung, M. S.-H.; Lam, Y.-W.; Lo, K. K.-W. *Inorg. Chem.* **2010**, *49*, 2530–2540. (k) Leung, S.-K.; Kwok, K. Y.; Zhang, K. Y.; Lo, K. K.-W. *Inorg. Chem.* **2010**, *49*, in press. (l) Li, S. P.-Y.; Liu, H.-W.; Zhang, K. Y.; Lo, K. K.-W. *Chem.—Eur. J.* **2010**, *16*, in press.

Chart 1. Structures of Polypyridine Ligands

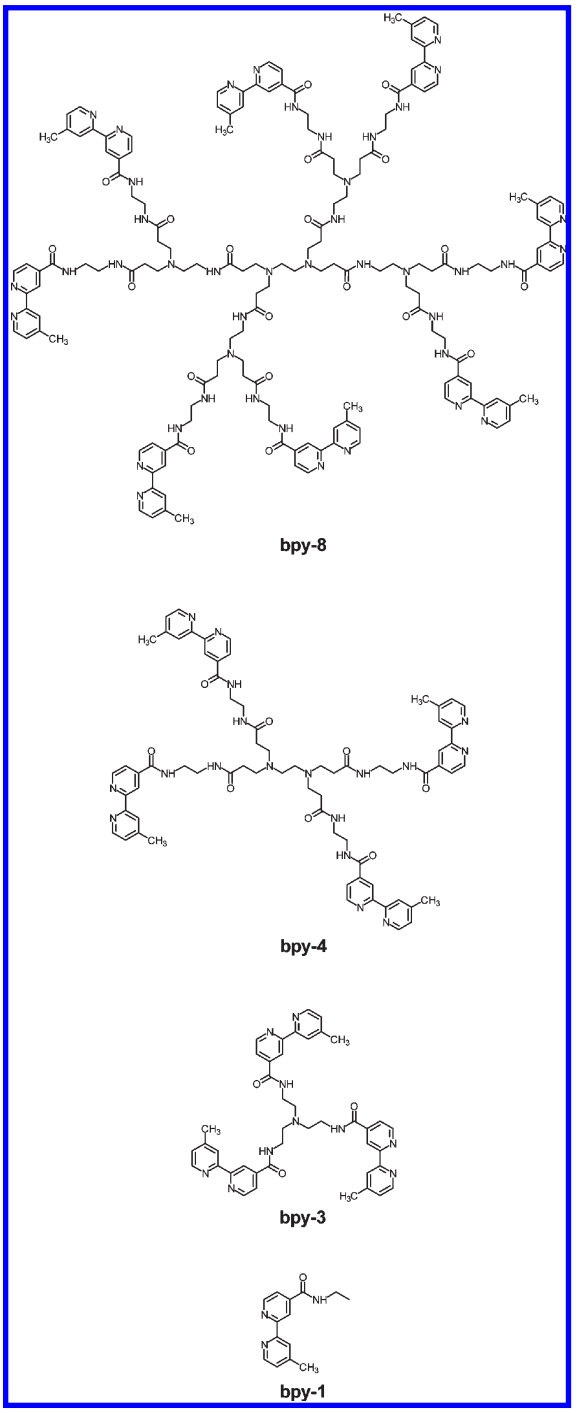

units are well documented, related studies on multinuclear complexes have not been explored. All these reasons have prompted us to design new luminescent dendritic cyclometalated iridium(III) polypyridine complexes and investigate their photophysical and biological properties. In particular, the effects of the lipophilicity, formal charge, and molecular size on the biological and cellular uptake properties of these complexes, and a comparison with their mononuclear counterparts are of much interest.

In this work, we report the synthesis and characterization of a series of luminescent dendritic cyclometalated iridium(III) polypyridine complexes $[\{Ir(N^{\wedge}C)_2\}_n(bpy\text{-}n)](PF_6)_n$ (HN^C = 2-phenylpyridine, Hppy, n = 8 (**ppy-8**), 4 (**ppy-4**), 3 (**ppy-3**); HN^C = 2-phenylquinoline, Hpq, n = 8 (**pq-8**), 4 (**pq-4**), 3 (**pq-3**)). The structures of the polypyridine ligands are shown in Chart 1. The properties of these dendrimers have been compared to those of their monomeric counterparts $[Ir(N^{\wedge}C)_2(bpy\text{-}1)](PF_6)$ (HN^C = Hppy (**ppy-1**), Hpq (**pq-1**)).[43g] The interaction of these complexes with plasmid DNA has been investigated by agarose gel retardation assays. The lipophilicity of all the complexes has been determined by reversed-phase high-performance liquid chromatography (HPLC). Additionally, the cellular uptake of the complexes by the human cervix epithelioid carcinoma (HeLa) cell line has been examined by inductively coupled plasma mass spectrometry (ICP-MS), laser-scanning confocal microscopy, and flow cytometry. Furthermore, the cytotoxicity of these iridium(III) complexes has been evaluated by the 3-(4,5-dimethyl-2-thiazolyl)-2,5-diphenyltetrazolium bromide (MTT) assay. The most important results are that the dendritic complexes showed interesting DNA-binding capabilities and a cellular uptake pathway that is different to their mononuclear counterparts. Also, these dendritic complexes bound to specific cellular compartments in HeLa cells, which has not been observed in the cellular uptake studies of related luminescent inorganic and organometallic transition metal complexes.

Results and Discussion

Synthesis. The bpy-terminated dendritic ligands **bpy-*n*** (n = 8, 4, 3) (Chart 1) were obtained from the reaction of amine-terminated dendrimers with bpy-NHS (1.5 equiv per terminal primary amine moiety) and triethylamine (1.5 equiv per terminal primary amine moiety) in dried *N*,*N*-dimethylformamide (DMF) at room temperature for 18 h. These ligands were purified by silica gel column chromatography and characterized by ^{1}H NMR spectroscopy and positive-ion electrospray ionization mass spectrometry (ESI-MS). The preparation of the dendritic iridium(III) complexes **ppy-*n*** and **pq-*n*** (n = 8, 4, 3) was accomplished by reacting the bpy-terminated dendritic ligands **bpy-*n*** (n = 8, 4, 3) with $[Ir_2(ppy)_4Cl_2]$ or $[Ir_2(pq)_4Cl_2]$ (0.5 equiv per terminal bpy moiety) in refluxing CH_2Cl_2/MeOH, followed by metathesis with KPF_6. The complexes were purified by silica gel column chromatography and recrystallized from CH_2Cl_2/diethyl ether to yield yellow to orange crystals. All the iridium(III) complexes were characterized by ^{1}H NMR spectroscopy, positive-ion ESI-MS, IR spectroscopy, and elemental analysis. Positive-ion ESI-MS was very useful in confirming the structures of these complexes. Consecutive loss of PF_6^- units and addition of H^+ were observed in all the spectra of the dendritic iridium(III) complexes. For example, the spectrum of complex **pq-4** was dominated by four peaks corresponding to $\{M + H^+ - PF_6^-\}^{2+}$, $\{M - 2 \times PF_6^-\}^{2+}$, $\{M + H^+ - 2 \times PF_6^-\}^{3+}$, and $\{M - 3 \times PF_6^-\}^{3+}$ ions. All the dendritic iridium(III) complexes were very soluble in common organic solvents such as CH_2Cl_2 and CH_3CN, and aqueous DMSO solution. However, they were only sparingly soluble in aqueous buffers.

Electrochemical Properties. The electrochemical properties of all the complexes have been studied by cyclic voltammetry. The electrochemical data are listed in Table 1. Similar to the monomeric complexes **ppy-1** and **pq-1** that showed a reversible iridium(IV/III) oxidation couple at about +1.27 V and a bipyridine-based reduction couple at about −1.28 V versus SCE, the dendritic complexes **ppy-*n***

and **pq-*n*** (n = 8, 4, 3) exhibited reversible couples at about +1.24 to +1.29 V and −1.21 to −1.27 V. These data indicate that there are negligible electronic communications between the [Ir(N^C)$_2$(N^N)] moieties in the same dendritic molecule. The reduction waves at potentials more negative than −1.7 V are quasi-reversible or highly irreversible in nature, and have been assigned to the reduction of the bipyridine and the cyclometalating ligands.

Electronic Absorption and Luminescence Properties. The electronic absorption spectral data of all the complexes are listed in Table 2. The electronic absorption spectra of complexes **pq-*n*** (n = 8, 4, 3, 1) in CH_3CN at 298 K are shown in Figure 1. All the complexes displayed intense absorption bands and shoulders at about 253−344 nm (ε on the order of 10^4 to 10^5 dm^3 mol^{-1} cm^{-1}), which have been assigned to spin-allowed intraligand (^{1}IL) ($\pi \rightarrow \pi^*$) (bpy-*n* and N^C) transitions. The less intense shoulders at > about 350 nm have been assigned to spin-allowed metal-to-ligand charge-transfer (^{1}MLCT) (dπ(Ir) → π^*-(bpy-*n* and N^C)) transitions. The weak absorption tailing at about 475−550 nm has been assigned to spin-forbidden ^{3}MLCT (dπ(Ir) → π^*(bpy-*n* and N^C)) transitions. As expected, the molar absorptivity of the dendritic iridium(III) complexes is approximately proportional to the number of [Ir(N^C)$_2$(N^N)] moieties in the complex molecule. The absorption profiles of the complexes containing the same N^C ligand are highly similar, further indicating that there are no electronic communications between the [Ir(N^C)$_2$(N^N)] moieties in the same dendritic complex molecule.

Table 1. Electrochemical Data of the Iridium(III) Complexes[a]

complex	oxidation, $E_{1/2}$/V	reduction, $E_{1/2}$ or E_c/V
ppy-8	+1.24	−1.27, −1.87,[b] −2.25,[c] −2.47[c]
ppy-4	+1.28	−1.26, −1.83,[b] −2.25,[c] −2.48[c]
ppy-3	+1.26	−1.27, −1.77,[b] −2.24,[c] −2.51[c]
ppy-1[d]	+1.26	−1.28, −1.84,[b] −2.27,[b] −2.48[b]
pq-8	+1.25	−1.22, −1.79,[b] −1.92,[c] −2.21[c]
pq-4	+1.28	−1.21, −1.72,[b] −1.90,[c] −2.21[c]
pq-3	+1.29	−1.22, −1.77,[b] −1.97,[c] −2.22[c]
pq-1[d]	+1.28	−1.28, −1.72,[b] −1.93,[b] −2.22[b]

[a] In CH_3CN (0.1 mol dm^{-3} ^{n}Bu$_4$NPF$_6$) at 298 K, glassy carbon electrode, sweep rate 100 mV s^{-1}, all potentials versus SCE. [b] Quasi-reversible couples. [c] Irreversible waves. [d] From reference 43g.

Upon photoexcitation, all the complexes displayed intense and long-lived greenish-yellow to orange luminescence in fluid solutions under ambient conditions and in low-temperature glass. The photophysical data are summarized in Table 3. The emission spectra of complexes **ppy-8** and **pq-8** in CH_3CN at 298 K are shown in Figure 2. For the ppy complexes, on going from relatively nonpolar CH_2Cl_2 to polar MeOH, they exhibited longer emission wavelengths, shorter emission lifetimes, and lower luminescence quantum yields (Table 3). Thus, the emission has been tentatively assigned to an excited state of ^{3}MLCT (dπ(Ir) → π^*(bpy-*n*)) character. Their emission maxima also displayed significant blue-shifts upon cooling the samples from room temperature to 77 K (Table 3), which is a common feature for cyclometalated iridium(III) polypyridine ^{3}MLCT emitters. Interestingly, in aqueous buffer at 298 K, the dendritic complexes **ppy-*n*** (n = 8, 4, 3) showed an unexpected shorter emission wavelength (λ_{em} = 588 to 594 nm) which is in contrast to the mononuclear complex **ppy-1** (λ_{em} = 625 nm). We have ascribed this to a more nonpolar local environment for the polynuclear complexes offered by the dendritic cores. The emission quantum yields in buffer followed the order: **ppy-1** < **ppy-3** ≈ **ppy-8** < **ppy-4**, which is in line with the trend of the emission wavelengths (Table 3). The more highly branched dendritic skeleton of complex **ppy-8** increases the flexibility of the complex, which may account for a lower quantum yield compared to that of complex

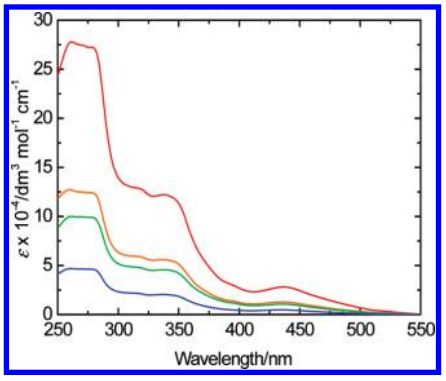

Figure 1. Electronic absorption spectra of complexes **pq-8** (red), **pq-4** (orange), **pq-3** (green), and **pq-1** (blue) in CH_3CN at 298 K.

Table 2. Electronic Absorption Spectral Data of the Iridium(III) Complexes at 298 K

complex	solvent	λ_{abs}/nm (ε/dm^3 mol^{-1} cm^{-1})
ppy-8	CH_2Cl_2	257 (388,410), 267 sh (368,135), 356 sh (68,030), 382 sh (59,890), 467 (8,150)
	CH_3CN	255 (347,240), 267 sh (323,130), 360 sh (57,210), 381 sh (49,860), 466 (6,840)
ppy-4	CH_2Cl_2	257 (197,740), 267 sh (185,170), 358 sh (33,705), 382 sh (30,345), 468 (3,975)
	CH_3CN	255 (174,720), 267 sh (160,105), 360 sh (29,365), 381 sh (25,930), 466 (3,460)
ppy-3	CH_2Cl_2	257 (146,095), 268 sh (136,135), 355 sh (35,865), 382 sh (31,930), 468 (4,150)
	CH_3CN	255 (123,735), 264 sh (115,075), 350 sh (22,665), 381 sh (18,585), 466 (2,490)
ppy-1[a]	CH_2Cl_2	256 (66,075), 271 sh (58,420), 320 sh (21,640), 339 sh (12,130), 361 sh (10,105), 384 (9,240), 413 sh (5,990), 464 sh (1,205)
	CH_3CN	253 (57,730), 268 sh (52,710), 318 sh (20,440), 336 sh (11,505), 358 sh (9,610), 381 (8,190), 416 sh (3,670), 476 sh (1,215)
pq-8	CH_2Cl_2	263 (336,940), 267 sh (335,585), 282 sh (334,480), 313 sh (160,780), 342 sh (150,970), 438 (35,230)
	CH_3CN	263 (277,455), 267 sh (275,025), 278 sh (273,875), 317 sh (126,135), 340 sh (119,150), 436 (25,910)
pq-4	CH_2Cl_2	263 (175,165), 267 sh (174,455), 278 sh (174,035), 313 sh (78,190), 342 sh (54,190), 438 (18,250)
	CH_3CN	263 (126,440), 267 sh (125,600), 278 sh (125,300), 317 sh (59,135), 339 sh (55,880), 434 (12,835)
pq-3	CH_2Cl_2	263 (139,185), 267 sh (138,715), 281 sh (139,100), 313 sh (67,030), 342 sh (63,200), 438 (14,465)
	CH_3CN	263 (99,750), 267 sh (99,285), 281 sh (97,215), 313 sh (47,425), 339 sh (44,155), 435 (10,050)
pq-1[a]	CH_2Cl_2	260 (56,110), 281 (54,440), 318 (24,090), 343 (23,300), 394 (5,700), 437 (5,510), 464 sh (3,620)
	CH_3CN	259 (46,610), 281 (45,490), 314 sh (21,680), 344 (19,470), 393 sh (4,860), 435 (4,800), 455 sh (3,600)

[a] From reference 43g.

Table 3. Photophysical Data of the Iridium(III) Complexes

complex	medium (T/K)	λ_{em}/nm	τ_o/μs	Φ_{em}
ppy-8	CH_2Cl_2 (298)	599	0.33	0.10
	CH_3CN (298)	613	0.18	0.036
	MeOH (298)	623	0.065	0.011
	buffer[a] (298)	592	0.14	0.0067
	glass[b] (77)	541, 580 sh	4.53	
ppy-4	CH_2Cl_2 (298)	603	0.26	0.081
	CH_3CN (298)	614	0.14	0.037
	MeOH (298)	620	0.061	0.023
	buffer[a] (298)	588	0.16	0.011
	glass[b] (77)	540, 576 sh	4.69	
ppy-3	CH_2Cl_2 (298)	597	0.34	0.10
	CH_3CN (298)	611	0.20	0.036
	MeOH (298)	620	0.066	0.015
	buffer[a] (298)	594	0.13	0.0061
	glass[b] (77)	541, 572 sh	4.75	
ppy-1	CH_2Cl_2[c] (298)	609	0.40	0.13
	CH_3CN[c] (298)	613	0.23	0.058
	MeOH (298)	619	0.10	0.015
	buffer[a] (298)	625	0.34	0.0023
	glass[b,c] (77)	541, 569 sh	4.80	
pq-8	CH_2Cl_2 (298)	554 sh, 587	0.45	0.11
	CH_3CN (298)	562, 592 sh	0.40	0.077
	MeOH (298)	557 sh, 608	0.11	0.019
	buffer[a] (298)	572, 601 sh	0.11	0.011
	glass[b] (77)	543 (max), 587	4.27	
pq-4	CH_2Cl_2 (298)	560 sh, 587	0.46	0.11
	CH_3CN (298)	560 sh, 587	0.34	0.096
	MeOH (298)	551 sh, 603	0.11	0.018
	buffer[a] (298)	567 sh, 597	0.10	0.0056
	glass[b] (77)	543 (max), 583	4.88	
pq-3	CH_2Cl_2 (298)	557, 599 sh	0.83	0.16
	CH_3CN (298)	557, 600 sh	0.46	0.078
	MeOH (298)	557, 599 sh	0.12	0.030
	buffer[a] (298)	563 sh, 597	0.13	0.0034
	glass[b] (77)	542 (max), 583	4.76	
pq-1	CH_2Cl_2[c] (298)	557 sh, 592	0.67	0.18
	CH_3CN[c] (298)	566, 606 sh	0.54	0.14
	MeOH (298)	570, 600 sh	0.22	0.026
	buffer[a] (298)	574, 596 sh	0.17	0.013
	glass[b,c] (77)	543 (max), 585	4.69	

[a] 50 mM potassium phosphate buffer pH 7.4/MeOH (9:1, v/v). [b] EtOH/MeOH (4:1, v/v). [c] From reference 43g.

ppy-4. The pq complexes showed two emission features at about 551−574 and 587−608 nm, respectively, in fluid solutions at 298 K (Table 3). Their emission maxima underwent a much smaller blue-shift upon cooling to 77 K compared to the ppy complexes, which is possibly a result of the mixing of some ^{3}IL ($\pi \rightarrow \pi^*$) (pq) character into their emissive state.[43a,e,g,h,j,l] In general, the dendritic complexes **ppy-*n*** and **pq-*n*** (n = 8, 4, 3) showed rather similar emission energies, quantum yields, and emission lifetimes at room temperature or 77 K compared to their monomeric counterparts **ppy-1** and **pq-1**, respectively, further supporting that the [Ir(C^N)$_2$(N^N)] units exhibit negligible electronic communications.

The emission quantum yields of these complexes in aqueous buffer were only moderate (Table 3), which is a typical feature for cyclometalated iridium(III) bipyridine-based ^{3}MLCT emitters.[43e,g−i,l] However, this is not considered a disadvantage as the most important requirement for luminescent probes in biological recognition and sensing applications is that they show strongly environment-sensitive emission. For example, the weak emission of ruthenium(II) and iridium(III) dppz and dpq complexes in aqueous solution does not hamper their interesting DNA and cellular sensing capabilities.[43c,j,44] In this work, there is a large difference between the emission quantum yields of the complexes in solvents of different polarity. Indeed, intracellular location of the complexes can be readily detected by laser-scanning confocal microscopy (see below), and thus, the low emission quantum yields in aqueous buffer are not a limitation for these iridium(III) complexes.

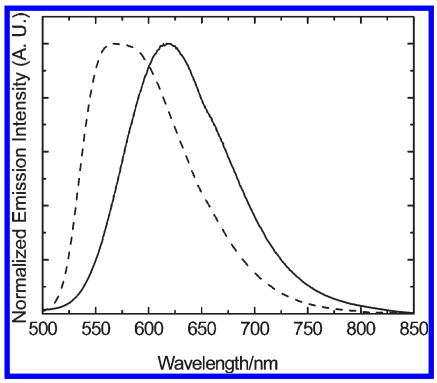

Figure 2. Emission spectra of complexes **ppy-8** (solid) and **pq-8** (dashed) in CH_3CN at 298 K.

DNA Interaction. Cationic dendrimers usually show good DNA condensation ability, and the association of these dendrimers with DNA results in the formation of dendriplexes.[45−47] We have studied the possible interaction of the iridium(III) complexes with DNA. Although addition of double-stranded calf thymus DNA to a solution of the complex in Tris-Cl buffer (50 mM, pH 7.4) did not cause any change to the absorption and emission spectra, the condensation of plasmid DNA (pDNA) by the complexes has been demonstrated by agarose gel retardation assays (Figure 3). It can be seen that complexes **ppy-8** and **pq-8** effectively formed dendriplexes with pDNA (1 μg) at [Ir] (concentration with respect to iridium) being as low as 12.5 nM whereas complexes **ppy-4**, **pq-4** and **ppy-3**, **pq-3** were slightly less potent and could only inhibit the migration of pDNA at [Ir] ≥ 25 and 100 nM, respectively. This implies that the interaction of these dendritic complexes with pDNA originates from electrostatic attraction. Another possible reason is the interaction of the dendritic motifs of the complexes with the biopolymer. In contrast, for the monomeric complexes **ppy-1** and **pq-1**, no obvious pDNA condensation was observed even at [Ir] = 400 nM, which is probably due to their lower cationic charge and the lack of dendritic skeleton.

Lipophilicity. The lipophilicity of a compound refers to its ability to dissolve in fats, oils, lipids, and nonpolar solvents, and is highly related to its efficiency to permeate biological membranes.[48] It is commonly estimated by the partition coefficient ($P_{o/w}$) in n-octanol/water.[49] The lipophilicity (log $P_{o/w}$) of the complexes in this work has

(44) (a) Puckett, C. A.; Barton, J. K. *J. Am. Chem. Soc.* **2007**, *129*, 46–47. (b) Puckett, C. A.; Barton, J. K. *Biochemistry* **2008**, *47*, 11711–11716.

(45) Navarro, G.; de ILarduya, C. T. *Nanomedicine* **2009**, *5*, 287–297.
(46) Mintzer, M. A.; Merkel, O. M.; Kissel, T.; Simanek, E. E. *New J. Chem.* **2009**, *33*, 1918–1925.
(47) Merkel, O. M.; Mintzer, M. A.; Sitterberg, J.; Bakowsky, U.; Simanek, E. E.; Kissel, T. *Bioconjugate Chem.* **2009**, *20*, 1799–1806.
(48) VanBrocklin, H. F.; Liu, A.; Welch, M. J.; O'Neil, J. P.; Katzenellenbogen, J. A. *Steroids* **1994**, *59*, 34–45.
(49) Minick, D. J.; Frenz, J. H.; Patrick, M. A.; Brent, D. A. *J. Med. Chem.* **1988**, *31*, 1923–1933.

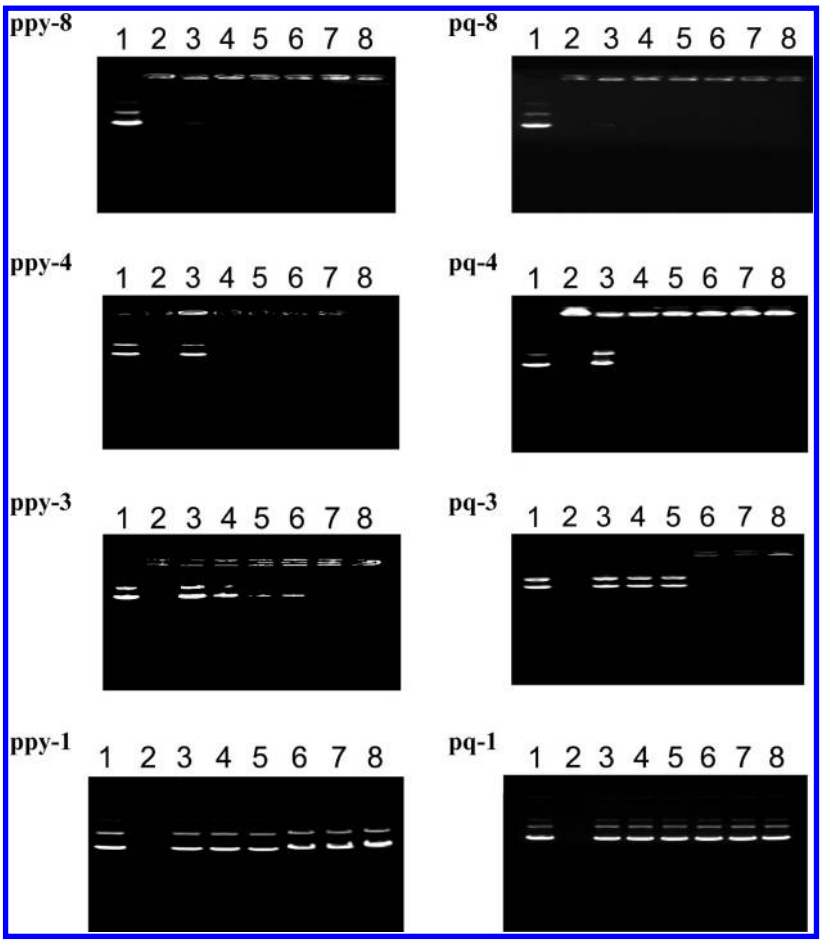

Figure 3. Results of agarose gel retardation assays of the iridium(III) complexes and plasmid DNA in PBS/DMSO (10 μL, 7:3, v/v). Lane 1: DNA (1 μg) only. Lane 2: the iridium(III) complex only. Lanes 3−8: DNA (1 μg) and the iridium(III) complex ([Ir] = 12.5, 25, 50, 100, 200, and 400 nM, respectively).

Table 4. Lipophilicity (log $P_{o/w}$) of the Iridium(III) Complexes

complex	log $P_{o/w}$
ppy-8	1.66
ppy-4	2.06
ppy-3	1.87
ppy-1[a]	0.44
pq-8	2.61
pq-4	3.40
pq-3	2.93
pq-1[a]	2.01

[a] From reference 43g.

Table 5. Numbers of Moles and Concentrations of Iridium Associated with an Average HeLa Cell upon Incubation with the Iridium(III) Complexes ([Ir] = 2 μM) at 37 °C for 2 h as Determined by ICP-MS

complex	number of mol/fmol	[Ir]/mM
ppy-8	0.65	0.19
ppy-4	0.95	0.28
ppy-3	0.98	0.29
ppy-1	3.8	1.1
pq-8	0.66	0.19
pq-4	0.94	0.26
pq-3	0.88	0.28
pq-1	7.1	2.1

been determined by reversed-phase HPLC, and the results are listed in Table 4. The log $P_{o/w}$ values of the pq complexes are larger than those of their corresponding ppy counterparts, resulting from the additional fused phenyl ring of the pq ligand. Interestingly, the lipophilicity of the dendritic complexes **ppy-*n*** (n = 8, 4, 3) (log $P_{o/w}$ = 1.66−2.06) and **pq-*n*** (n = 8, 4, 3) (log $P_{o/w}$ = 2.61−3.40) is substantially higher than that of the monomeric complexes **ppy-1** (log $P_{o/w}$ = 0.44) and **pq-1** (log $P_{o/w}$ = 2.01), respectively, reflecting the hydrophobic nature of the dendritic skeleton moiety. This is in accordance with the observation that the tetranuclear complexes **ppy-4** and **pq-4** showed larger log $P_{o/w}$ values (2.06 and 3.40, respectively) than the corresponding trinuclear complexes **ppy-3** and **pq-3** (log $P_{o/w}$ = 1.87 and 2.93, respectively). However, complexes **ppy-8** and **pq-8** exhibited the lowest lipophilicity (log $P_{o/w}$ = 1.66 and 2.61, respectively) among all the dendritic complexes, which may be a consequence of the polar amine and amide groups and the +8 formal charge.

Cellular Uptake. The cellular uptake of the complexes has been studied by ICP-MS measurements. The amounts and concentrations of iridium associated with HeLa cells incubated with the complexes ([Ir] = 2 M) at 37 °C for 2 h are listed in Table 5. An average cell (mean volume of 3.4 pL) contained 0.65 to 7.1 fmol of iridium, which is comparable to those reported in the cellular uptake studies of iridium[43i,l] and other inorganic complexes.[50−53]

(50) Brunner, J.; Barton, J. K. *Biochemistry* **2006**, *45*, 12295–12302.
(51) Yu, J.; Parker, D.; Pal, R.; Poole, R. A.; Cann, M. J. *J. Am. Chem. Soc.* **2006**, *128*, 2294–2299.

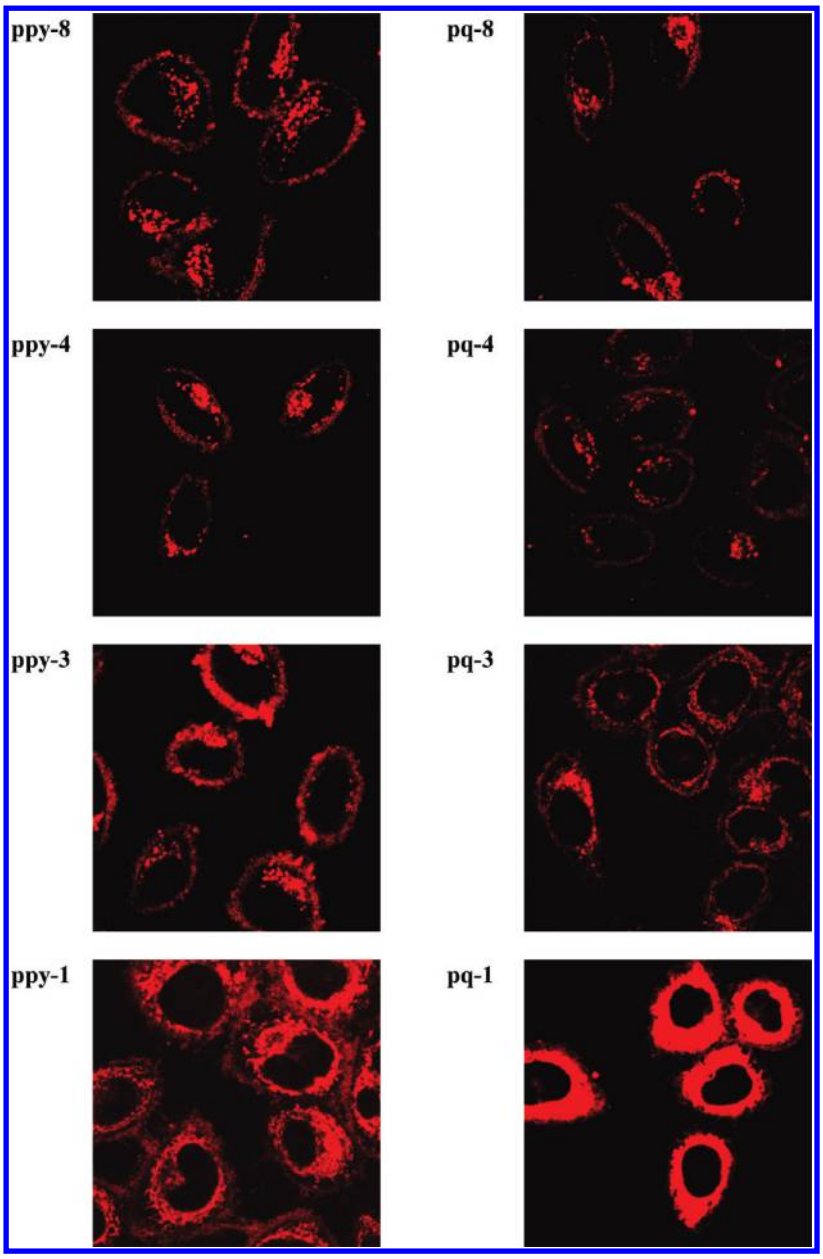

Figure 4. Laser-scanning confocal microscopy images of HeLa cells incubated with the iridium(III) complexes ([Ir] = 2 μM) at 37 °C for 2 h.

The dendritic complexes exhibited a lower cellular uptake efficiency (approximately one order of magnitude lower in terms of [Ir]) compared to the monomeric complexes, probably because of their higher cationic charge and much larger molecular size. The monomeric pq complex **pq-1** displayed almost a double cellular uptake efficiency ([Ir] = 2.1 mM) compared to that of complex **ppy-1** ([Ir] = 1.1 mM), which can be ascribed to the higher lipophilicity of the former complex (Table 4). However, the dendritic pq complexes **pq-*n*** (n = 3, 4, 8), despite their higher lipophilicity, showed similar cellular uptake efficiencies compared to their corresponding ppy counterparts **ppy-*n*** (n = 3, 4, 8). This illustrates that, regarding cellular uptake efficiency of the dendritic complexes, the branched skeletons play a more important role compared to the cyclometalating ligands. It is important to point out that the [Ir] of all the complexes (0.19−2.1 mM, Table 5) are much higher than that of the free complexes in the medium before the uptake (2 μM), indicating that the complexes were concentrated within the cells. However, the measured concentrations indicate iridium associated with the cells, which is not necessary all being in the interior. Thus, the data can only serve as an approximate indicator for cellular uptake efficiencies.

Confocal Imaging and Flow Cytometry. The internalization and intracellular localization of all the complexes have been investigated using laser-scanning confocal microscopy. The fluorescence microscopy images of HeLa cells treated with the complexes ([Ir] = 2 μM) for 2 h are illustrated in Figure 4. We found that the monomeric complexes **ppy-1** and **pq-1** were localized in

(52) Chauvin, A.-S.; Comby, S.; Song, B.; Vandevyver, C. D. B.; Bünzli, J.-C. G. *Chem.—Eur. J.* **2008**, *14*, 1726–1739.
(53) Louie, M.-W.; Liu, H.-W.; Lam, M. H.-C.; Lau, T.-C.; Lo, K. K.-W. *Organometallics* **2009**, *28*, 4297–4307.

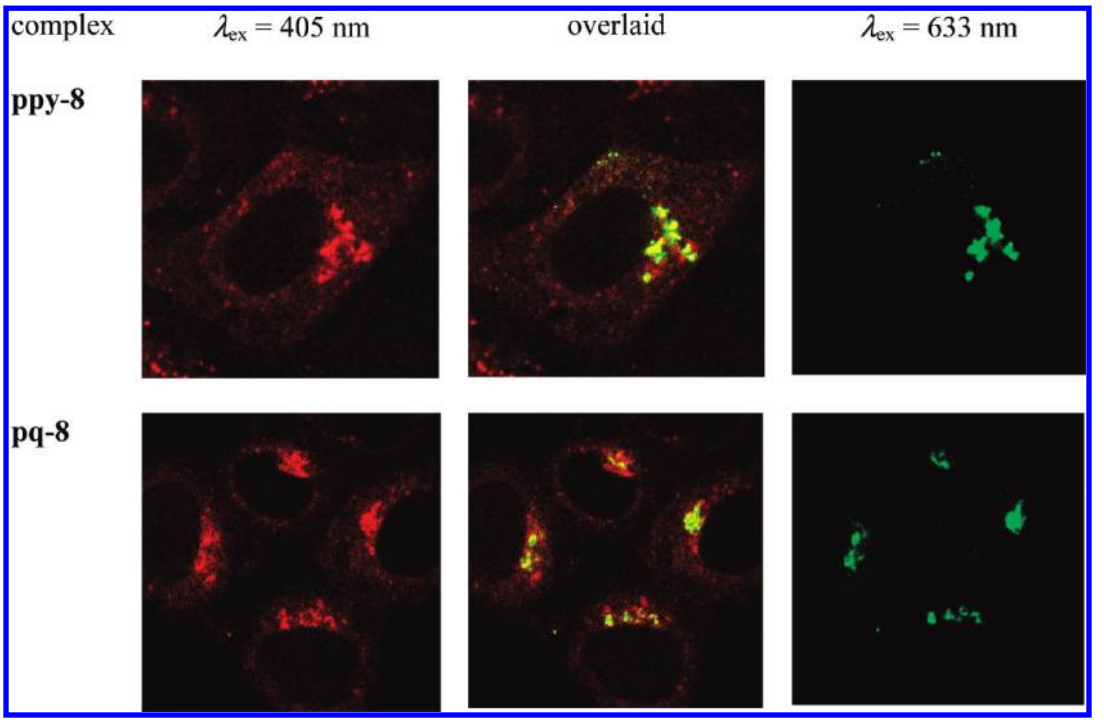

Figure 5. Laser-scanning confocal microscopy images of HeLa cells treated successively with complexes **ppy-8** or **pq-8** ([Ir] = 2 M) at 37 °C for 2 h, PBS containing 3% paraformaldehyde, anti-golgin-97 (human) mouse IgG_1 (1 μg/mL, 1 h), and Alexa 635 goat anti-mouse IgG (H+L) (10 μg/mL, 30 min).

Table 6. Mean Emission Intensities of HeLa Cells Incubated with Blank Medium and the Iridium(III) Complexes at 37 and 4 °C for 2 h as Determined by Flow Cytometry

	emission intensity after incubation	
complex	at 37 °C	at 4 °C
ppy-8	18.5	3.0
ppy-4	19.1	3.2
ppy-3	18.1	3.7
ppy-1	33.5	4.8
pq-8	15.9	3.0
pq-4	31.6	3.4
pq-3	53.7	3.9
pq-1	1641.3	625.3
blank medium	3.0	3.0

the perinuclear region, forming very sharp luminescent rings surrounding the nuclei. *Z*-scans of the cells confirmed that the complexes were indeed located inside the cells (Supporting Information, Figure S1). Similar intracellular distributions are commonly observed for other iridium(III) complexes.[38b,43g−i,k,l] However, in addition to the perinuclear region, the dendritic complexes also bound to specific compartments of the cells, which are likely to be the Golgi apparatus (Figure 4). This has been confirmed by co-staining experiments using complexes **ppy-8** and **pq-8** as examples. Specifically, HeLa cells treated with complexes **ppy-8** and **pq-8**, respectively, were fixed and incubated with anti-golgin-97 (human) mouse IgG_1 (1 μg/mL, 1 h), and subsequently stained by Alexa 635 goat anti-mouse IgG (H+L) (10 μg/mL, 30 min). The dye Alexa 635 was used because its spectral properties do not interfere with those of the iridium(III) complexes. It can be seen in Figure 5 that the Golgi apparatus has been co-stained by the complexes and the fluorescent antibody.

The cellular uptake has been investigated by temperature-dependence experiments and analyzed by flow cytometry.

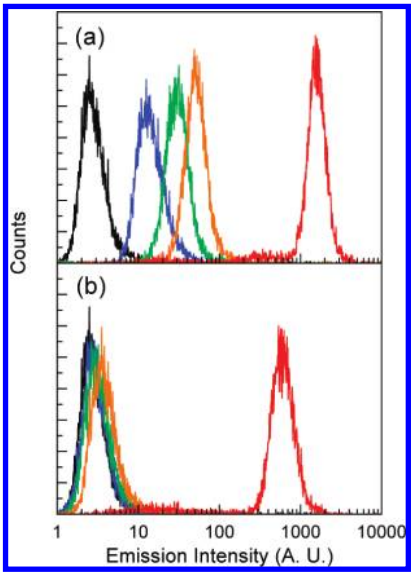

Figure 6. Flow cytometric results of HeLa cells incubated with blank medium (black) and complexes **pq-8** (blue), **pq-4** (green), **pq-3** (orange), and **pq-1** (red) at (a) 37 °C and (b) 4 °C for 2 h.

The mean emission intensities of HeLa cells incubated with all the complexes and blank medium at 37 and 4 °C are presented in Table 6. All the cell samples incubated with the complexes at 37 °C displayed emission intensities that are higher than the autofluorescence of untreated HeLa cells, reflecting efficient cellular uptake of the complexes. The emission intensities of HeLa cells treated with the dendritic ppy complexes **ppy-*n***, (n = 8, 4, 3) at 37 °C are similar to each other and lower than those incubated with their monomeric counterpart **ppy-1** (Table 6). For the pq complexes at 37 °C, the emission intensities increased with a decreasing number of $[Ir(pq)_2(N^{\wedge}N)]$ moieties and followed

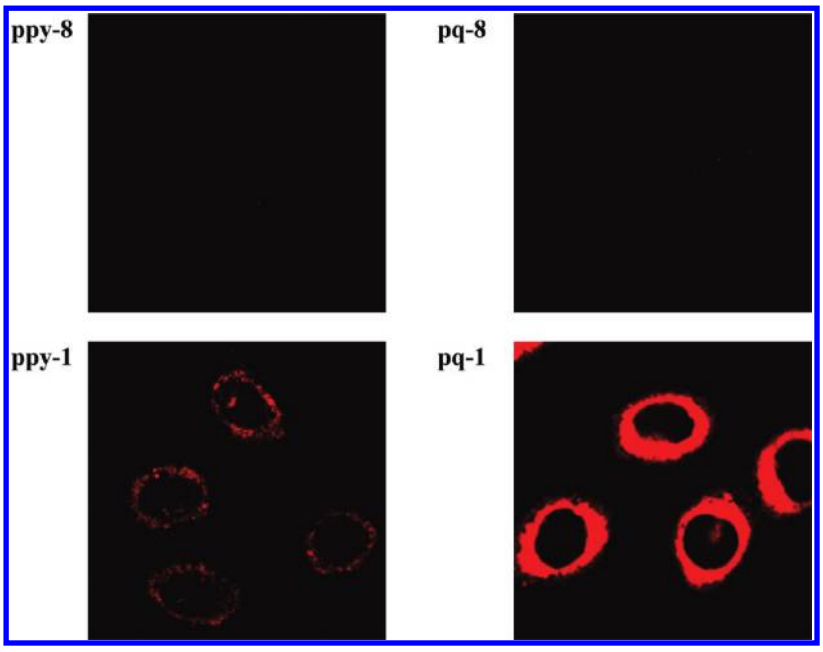

Figure 7. Laser-scanning confocal microscopy images of HeLa cells incubated with complexes **ppy-8**, **ppy-1**, **pq-8**, and **pq-1** ([Ir] = 2 μM) at 4 °C for 2 h.

the order: **pq-8** < **pq-4** < **pq-3** ≪ **pq-1** (Table 6 and Figure 6a). Upon lowering the incubation temperature to 4 °C, the emission intensities of HeLa cells treated with all the complexes were reduced (Table 6). The cells treated with the dendritic complexes **ppy-*n*** and **pq-*n*** (n = 8, 4) became hardly emissive, whereas the cells loaded with complex **ppy-1** showed a small but noticeable emission intensity and those incubated with complex **pq-1** still displayed rather strong luminescence (Table 6 and Figure 6b). These results are consistent with the confocal microscopy images of HeLa cells treated with the dendritic complexes **ppy-8** and **pq-8** at 4 °C, which did not reveal luminescence (Figure 7). In contrast, cells loaded with the monomeric complexes **ppy-1** and **pq-1** at 4 °C were emissive, with the latter complex giving very strong emission intensity (Figure 7 and Supporting Information, Figure S1). All these results indicate that the dendritic complexes entered the cells by an energy-dependent process (which is likely to be endocytosis), whereas an energy-independent diffusion-like mechanism also occurred for the monomeric complexes, especially for complex **pq-1**. The coexistence of these cellular internalization pathways has been observed for other cyclometalated iridium(III) complexes.[43i] It is conceivable that the different internalization pathways and localizations between the dendritic and mononuclear complexes originate from the different formal charge and molecular size of the complexes, and the dendritic skeletons also play a role in the cellular uptake properties.[54]

Cytotoxicity. The cytotoxicity of the complexes toward the HeLa cell line has been studied by the MTT assay.[55] The dose dependence of surviving cells after exposure to the complexes for 48 h has been evaluated, and the IC_{50} values are shown in Table 7. The iridium(III) complexes showed higher or comparable cytotoxicity (IC_{50} = 1.4 to 26.4 μM) compared to cisplatin (IC_{50} = 26.4 μM) under the same experimental conditions. In general, from our previous work, we found that there is a correlation between the lipophilicity and cytotoxicity of this type of complexes, with higher lipophilicity resulting in higher cytotoxicity.[43g−l] This relationship has also been observed in this work: the IC_{50} values of the pq complexes are smaller than those of their corresponding ppy counterparts, indicative of higher cytotoxicity related to the more hydrophobic pq ligand (Table 7). To illustrate the effects of the dendritic structure of the complexes on their cytotoxicity, the IC_{50} values are also presented in terms of [Ir] (Table 7). The dendritic ppy complex **ppy-8** (IC_{50} = 16.8 μM) is slightly more cytotoxic than its monomeric counterpart **ppy-1** (IC_{50} = 26.4 μM). However, the reverse was observed for the **pq** analogues: the cytotoxicity of complex **pq-8** (IC_{50} = 11.2 μM) is apparently lower than that of complex **pq-1** (IC_{50} = 5.5 μM).

Table 7. Cytotoxicity (IC_{50}, 48 h) of the Iridium(III) Complexes and Cisplatin Toward the HeLa Cell Line

complex	IC_{50} [complex]/μM	IC_{50} [Ir]/μM
ppy-8	2.1 ± 0.2	16.8 ± 1.6
ppy-4	3.3 ± 0.1	13.2 ± 0.4
ppy-3	5.2 ± 0.3	15.6 ± 0.9
ppy-1	26.4 ± 3.4	26.4 ± 3.4
pq-8	1.4 ± 0.1	11.2 ± 0.8
pq-4	2.1 ± 0.1	8.4 ± 0.4
pq-3	2.7 ± 0.1	8.1 ± 0.3
pq-1	5.5 ± 0.7	5.5 ± 0.7
cisplatin	26.4 ± 2.0	N.A.

For the monomeric complexes, complex **pq-1** is about 5 times more cytotoxic than complex **ppy-1** (Table 7). We believe that the observed cytotoxicity is associated with the lipophilicity of the complex because **pq-1** is much more lipophilic (log $P_{o/w}$ = 2.01) than **ppy-1** (log $P_{o/w}$ = 0.44, Table 4). This is also in agreement with much higher membrane-permeability and hence higher cellular uptake efficiency of the former complex by passive diffusion (Table 5), for which the lipophilicity plays a very

(54) The possibility of aggregation of the dendritic complexes in aqueous solutions has been eliminated by light-scattering experiments, and we did not have evidence that the lack of passive diffusion of these complexes was due to aggregation.

(55) Mosmann, T. *J. Immunol. Methods* **1983**, *65*, 55–63.

important role. The IC_{50} values of the dendritic complexes **ppy-8** and **pq-8** are similar (16.8 and 11.2 μM, respectively, Table 7). Interestingly, their cellular uptake efficiencies are also very similar, and the intracellular [Ir] are lower than those of their monomeric counterparts by one order of magnitude (Table 5). We have attributed the different cytotoxicity of the monomeric complexes and their dendritic counterparts to a shift of the cellular uptake mechanism from essentially a passive-diffusion mode for the monomers to an energy-requiring endocytosis pathway for the dendrimers (see above). It is likely that these findings are a consequence of an increase of the formal charge, molecular size, and molecular weight of the dendritic complexes. In summary, we believe that the cytotoxicity of the complexes in this work originates primarily from their binding to organelles, in particular, the Golgi apparatus. Thus, higher cellular uptake efficiency results in higher cytotoxicity. While the uptake efficiency (and hence cytotoxicity) is strongly dependent on the lipophilicity of the mononuclear complexes which are internalized via essentially a passive diffusion pathway, it is less important to the polynuclear complexes because the dendritic cores play a more important role on the properties of the complexes and the uptake mechanism is energy-requiring endocytosis which is less dependent on the lipophilicity of the complexes.

Conclusion

In this work, dendrimers containing terminal luminescent cyclometalated iridium(III) polypyridine complexes have been synthesized and characterized. Their electrochemical and photophysical properties have been investigated. The results revealed that there are no electronic communications between the $[Ir(N^{\wedge}C)_2(N^{\wedge}N)]$ moieties in the same dendritic molecule. Agarose gel retardation assays showed that all the dendritic iridium(III) complexes, in contrast to their mononuclear counterparts, exhibited DNA condensation ability. Additionally, the lipophilicity, cellular uptake properties, and cytotoxicity of the complexes have been examined. Treatment of HeLa cells with the complexes resulted in localization in the perinuclear regions. Interstingly, cells loaded with the dendritic complexes also displayed Golgi staining, which is a novel finding. While the dendritic complexes are internalized essentially by an energy-dependent process, the mononuclear complexes exhibit an additional passive-diffusion pathway. These differences are most likely due to factors such as formal charge and molecular size. In conclusion, the luminescent dendritic cyclometalated iridium(III) polypyridine complexes in this work not only show favorable photophysical characteristics that are common to iridium(III) complexes but also exhibit interesting DNA condensation properties and intracellular localization. Studies of related dendrimers of higher generations containing luminescent inorganic and organometallic complexes are underway.

Experimental Section

Materials and Synthesis. All solvents were of analytical reagent grade and purified according to standard procedures.[56] All buffer components were of biological grade and used as received. $IrCl_3 \cdot 3H_2O$, Hppy, Hpq, 4,4′-dimethyl-2,2′-bipyridine, tris(2-aminoethyl)amine, PAMAM dendrimers (generations 0 and 1), *n*-octanol, 4-methoxyaniline, 4-methoxyphenol, phenol, acetophenone, naphthalene, *tert*-butylbenzene, anthracene, and pyrene were purchased from Aldrich. *N*-Hydroxysuccinimide, *N*,*N*′-dicyclohexylcarbodiimide, triethylamine, KPF_6, cisplatin, and paraformaldehyde were purchased from Acros. MTT was purchased from Sigma. Double-stranded calf thymus DNA was obtained from Calbiochem. PmCherry-C1 vector (4722 bp) was procured from Clontech. 4-Succinimidyl-carboxy-4′-methyl-2,2′-bipyridine,[57] the precursor complexes $[Ir_2(ppy)_4Cl_2]$[25a] and $[Ir_2(pq)_4Cl_2]$,[25a] and the monomeric complexes **ppy-1** and **pq-1**[43g] were prepared according to reported procedures. Tetra-*n*-butylammonium hexafluorophosphate (TBAP) was obtained from Aldrich and was recrystallized from hot ethanol and dried in vacuo at 110 °C before use. HeLa cells were obtained from American Type Culture Collection. Dulbecco's modified Eagle's medium (DMEM), fetal bovine serum (FBS), phosphate buffered saline (PBS), trypsin-EDTA, penicillin/streptomycin, anti-golgin-97 (human), mouse IgG_1, and Alexa 635 goat anti-mouse IgG (H+L) were purchased from Invitrogen. The growth medium for cell culture contained DMEM with 10% FBS and 1% penicillin/streptomycin.

bpy-8. A 20 wt % MeOH solution of PAMAM dendrimer, generation 1 (306 μL, 0.035 mmol) was evaporated to dryness under vacuum for 2 h. The resulting residue was dissolved in a mixture of DMF (3 mL) and triethylamine (163 μL, 1.16 mmol). To that solution was added 4-succinimidyl-carboxy-4′-methyl-2,2′-bipyridine (120 mg, 0.38 mmol) in DMF (2 mL). The reaction mixture was stirred at room temperature for 48 h, and then the DMF was removed under vacuum. The residue was purified by column chromatography on silica gel. The desired product was eluted with CH_2Cl_2/MeOH (6:1, v/v). The ligand **bpy-8** was subsequently isolated as a colorless oil. Yield: 80 mg (76%). ^{1}H NMR (300 MHz, $CDCl_3$, 298 K, TMS): δ 8.72 (br, 8H, CONH), 8.62−8.57 (m, 16H, H3 and H6 of bpy), 8.34 (d, 8H, J = 4.5 Hz, H6′ of bpy), 8.27 (br, 8H, CONH), 8.20−8.04 (m, 12H, CONH and H3′ of bpy), 7.64 (d, 8H, J = 4.5 Hz, H5 of bpy), 7.02 (d, 8H, J = 4.5 Hz, H5′ of bpy), 3.53−3.44 (m, 32H, $CONHCH_2$), 3.20−2.60 (m, 44H, $CONHCH_2$ and NCH_2), 2.54−2.33 (m, 48H, CH_2CO and CH_3 on C4′ of bpy).

bpy-4. A 20 wt % MeOH solution of PAMAM dendrimer, generation 0 (141 μL, 0.047 mmol) was evaporated to dryness under vacuum for 2 h. The resulting residue was dissolved in a mixture of DMF (5 mL) and triethylamine (108 μL, 0.77 mmol). To that solution was added 4-succinimidyl-carboxy-4′-methyl-2,2′-bipyridine (0.26 mmol, 80 mg) in DMF (2 mL). The reaction mixture was stirred at room temperature for 48 h, and then DMF was removed under vacuum. The residue was purified by column chromatography on silica gel. The desired product was eluted with CH_2Cl_2/MeOH (6:1, v/v). The ligand **bpy-4** was subsequently isolated as a colorless oil. Yield: 50 mg (82%). ^{1}H NMR (300 MHz, $CDCl_3$, 298 K, TMS): δ 8.66−8.57 (m, 12H, CONH, H3 and H6 of bpy), 8.36−8.34 (m, 8H, CONH, H6′of bpy), 8.07 (s, 4H, H3′ of bpy), 7.62 (d, 4H, J = 5.1 Hz, H5 of bpy), 7.06 (d, 4H, J = 5.1 Hz, H5′ of bpy), 3.53 (br, 8H, $CONHCH_2$), 3.43 (br, 8H, CH_2NHCO), 2.76 (br, 8H, NCH_2), 2.40−2.36 (m, 24H, NCH_2, CH_2CO and CH_3 on C4′ of bpy). Positive-ion ESI-MS ion cluster at m/z 1302 $\{M + H^+\}^+$.

bpy-3. A mixture of 4-succinimidyl-carboxy-4′-methyl-2,2′-bipyridine (0.23 mmol, 70 mg,), tris(2-aminoethyl)amine (8.4 μL, 0.056 mmol), and triethylamine (95 μL, 0.68 mmol) in DMF (5 mL) was stirred at room temperature for 12 h. The colorless solution was then evaporated to dryness under vacuum. The residue was purified by column chromatography on silica gel. The desired product was eluted with CH_2Cl_2/MeOH (6:1, v/v). The ligand **bpy-3** was subsequently isolated as a colorless oil. Yield: 40 mg (93%). ^{1}H NMR (300 MHz, CD_3OD, 298 K, TMS):

(56) Perrin, D. D.; Armarego, W. L. F. *Purification of Laboratory Chemicals*; Pergamon: Oxford, 1997.
(57) Telser, J.; Cruickshank, K. A.; Schanze, K. S.; Netzel, T. L. *J. Am. Chem. Soc.* **1989**, *111*, 7221–7226.

δ 8.30−8.29 (m, 6H, H3 and H6 of bpy), 8.22 (d, 3H, J = 4.8 Hz, H6′ of bpy), 7.81 (s, 3H, H3′ of bpy), 7.37 (d, 3H, J = 5.1 Hz, H5 of bpy), 7.03 (d, 3H, J = 4.8 Hz, H5′ of bpy), 3.44 (t, 6H, J = 5.7 Hz, CONHCH_2), 2.70 (t, 6H, J = 5.7 Hz, NCH_2), 2.24 (s, 9H, CH_3 on C4′ of bpy). Positive-ion ESI-MS ion cluster at m/z 736 $\{M + H^+\}^+$.

[{Ir(ppy)$_2$}$_8$(bpy-8)](PF$_6$)$_8$ (ppy-8). A mixture of [Ir$_2$(ppy)$_4$Cl$_2$] (139 mg, 0.11 mmol) and the ligand **bpy-8** (80 mg, 0.027 mmol) in CH_2Cl_2/MeOH (20 mL, 1:1, v/v) was refluxed under nitrogen for 4 h. The solution was then cooled to room temperature, and KPF_6 (79 mg, 0.43 mmol) was added to the solution. The mixture was then evaporated to dryness. The solid was dissolved in CH_2Cl_2/MeOH and purified by column chromatography on silica gel. The product was eluted with CH_2Cl_2/MeOH (10:1, v/v) and subsequently recrystallized from a mixture of CH_2Cl_2 and diethyl ether as yellow crystals. Yield: 47 mg (22%). ^{1}H NMR (300 MHz, $(CD_3)_2CO$, 298 K, TMS): δ 9.34 (br, 8H, H3 of bpy), 8.97 (br, 8H, H3′ of bpy), 8.17−8.02 (m, 36H, CONH, H6 of bpy, and H3 of pyridyl ring of ppy), 7.85−7.66 (m, 72 H, H5 and H6′ of bpy, H3 of phenyl ring and H4 and H6 of pyridyl ring of ppy, and CONH), 7.46 (br, 8H, H5′ of bpy), 7.11−6.83 (m, 48H, H5 of pyridyl ring of ppy, H4 and H5 of phenyl ring of ppy), 6.29 (br, 16H, H6 of phenyl ring of ppy), 3.41−3.29 (m, 40H, CONHCH_2, CH_2NHCO, CONHCH_2), 2.62−2.49 (m, 36H, NCH_2, CH_2N), 2.40−2.08 (m, 48H, CH_2CO, CH_3 on C4′ of bpy). Positive-ion ESI-MS ion cluster at m/z 2722 $\{M + 3 \times H^+\}^{3+}$, 2674 $\{M + 2 \times H^+ - PF_6^-\}^{3+}$, 2625 $\{M + H^+ - 2 \times PF_6^-\}^{3+}$, 2576 $\{M - 3 \times PF_6^-\}^{3+}$, 2043 $\{M + 4 \times H^+\}^{4+}$, 1999 $\{M + 3 \times H^+ - PF_6^-\}^{4+}$, 1970 $\{M + 2 \times H^+ - 2 \times PF_6^-\}^{4+}$, 1933 $\{M + H^+ - 3 \times PF_6^-\}^{4+}$, 1896 $\{M - 4 \times PF_6^-\}^{4+}$. IR (KBr) ν/cm^{-1}: 3425 (s, br, N−H), 1655 (s, C═O), 845 (s, PF_6^-). Anal. Calcd for $Ir_8C_{334}H_{320}N_{58}O_{20}P_8F_{48}\cdot 2CH_2Cl_2\cdot 2H_2O$: C, 48.22; H, 3.95; N, 9.71. Found: C, 48.16; H, 4.23; N, 9.92.

[{Ir(ppy)$_2$}$_4$(bpy-4)](PF$_6$)$_4$ (ppy-4). The procedure was similar to that for the preparation of complex **ppy-8**, except that **bpy-4** was used instead of **bpy-8**. Subsequent recrystallization from CH_2Cl_2/diethyl ether afforded complex **ppy-4** as yellow crystals. Yield: 40%. ^{1}H NMR (300 MHz, $(CD_3)_2CO$, 298 K, TMS): δ 9.02 (s, 4H, H3 of bpy), 8.69 (s, 4H, H3′ of bpy), 8.37 (br, 4H, CONH), 8.21−8.13 (m, 12H, H6 of bpy and H3 of pyridyl ring of ppy), 7.89−7.78 (m, 32H, H5 and H6′ of bpy and H3 of phenyl ring and H4 and H6 of pyridyl ring of ppy), 7.65 (br, 4H, CONH), 7.49 (d, 4H, J = 5.7 Hz, H5′ of bpy), 7.15−6.83 (m, 24H, H5 of pyridyl ring and H4 and H5 of phenyl ring of ppy), 6.31 (t, 8H, J = 5.7 Hz, H6 of phenyl ring of ppy), 3.43 (br, 8H, CONHCH_2), 3.37 (br, 8H, CH_2NHCO), 3.10 (br, 8H, NCH_2), 2.64−2.60 (m, 12H, CH_2N and CH_2CO), 2.52 (s, 12H, CH_3 on C4′ of bpy). Positive-ion ESI-MS ion cluster at m/z 1797 $\{M - 2 \times PF_6^-\}^{2+}$, 1150 $\{M - 3 \times PF_6^-\}^{3+}$, 826 $\{M - 4 \times PF_6^-\}^{4+}$. IR (KBr) ν/cm^{-1}: 3424 (s, br, N−H), 1656 (s, C═O), 845 (s, PF_6^-). Anal. Calcd for $Ir_4C_{158}H_{144}N_{26}O_8P_4F_{24}\cdot 4CH_2Cl_2$: C, 46.07; H, 3.63; N, 8.62. Found: C, 46.00; H, 3.76; N, 8.83.

[{Ir(ppy)$_2$}$_3$(bpy-3)](PF$_6$)$_3$ (ppy-3). The procedure was similar to that for the preparation of complex **ppy-8**, except that **bpy-3** was used instead of **bpy-8**. Subsequent recrystallization from CH_2Cl_2/diethyl ether afforded complex **ppy-3** as yellow crystals. Yield: 43%. ^{1}H NMR (300 MHz, $(CD_3)_2CO$, 298 K, TMS): δ 9.11 (s, 3H, H3 of bpy), 8.72 (s, 3H, H3′ of bpy), 8.42 (br, 3H, CONH), 8.23−8.18 (m, 6H, H3 of pyridyl ring of ppy), 8.08 (d, 3H, J = 5.7 Hz, H6 of bpy), 7.93−7.76 (m, 24H, H5 and H6′ of bpy and H3 of phenyl ring and H4 and H6 of pyridyl ring of ppy), 7.47 (d, 3H, J = 5.7 Hz, H5′ of bpy), 7.12−6.83 (m, 18H, H5 of pyridyl ring and H4 and H5 of phenyl ring of ppy), 6.31 (t, 6H, J = 5.7 Hz, H6 of phenyl ring of ppy), 3.55 (br, 6H, CONHCH_2), 2.84 (br, 6H, NCH_2), 2.42 (s, 9H, CH_3 on C4′ of bpy). Positive-ion ESI-MS ion cluster at m/z 2527 $\{M - PF_6^-\}^+$, 1191 $\{M - 2 \times PF_6^-\}^{2+}$. IR (KBr) ν/cm^{-1}: 3427 (s, br, N−H), 1661 (s, C═O), 845 (s, PF_6^-). Anal. Calcd for $Ir_3C_{108}H_{90}N_{16}O_3P_3F_{18}\cdot H_2O$: C, 48.23; H, 3.45; N, 8.33. Found: C, 47.93; H, 3.61; N, 8.63.

[{Ir(pq)$_2$}$_8$(bpy-8)](PF$_6$)$_8$ (pq-8). The procedure was similar to that for the preparation of complex **ppy-8**, except that [Ir$_2$(pq)$_4$Cl$_2$] was used instead of [Ir$_2$(ppy)$_4$Cl$_2$]. Subsequent recrystallization from CH_2Cl_2/diethyl ether afforded complex **pq-8** as orange crystals. Yield: 24%. ^{1}H NMR (300 MHz, $(CD_3)_2CO$, 298 K, TMS): δ 8.75 (br, 12H, CONH), 8.53−8.41 (m, 56H, H3, H3′, and H6 of bpy and H3 of quinoline and H3 of phenyl ring of pq), 8.23 (d, 8H, J = 8.1 Hz, H5 of bpy), 8.17−8.12 (m, 16H, H4 of quinoline of pq), 8.03−8.01 (m, 8H, H6′ of bpy), 7.84−7.77 (m, 24H, H8 of quinoline of pq, CONH), 7.51−7.49 (m, 8H, H5′ of bpy), 7.39−7.28 (m, 32H, H5, H7 of quinoline of pq), 7.18−7.03 (m, 32H, H4 of phenyl ring and H6 of quinoline of pq), 6.76−6.68 (m, 8H, H5 of phenyl ring of pq), 6.67 (br, 8H, H5 of phenyl ring of pq), 6.50−6.48 (m, 16H, H6 of phenyl ring of pq), 3.41−3.29 (m, 40H, CONHCH_2, CH_2NHCO, and CONHCH_2), 2.58−2.46 (m, 36H, NCH_2 and CH_2N), 2.31−2.21 (m, 48H, CH_2CO and CH_3 on C4′ of bpy). Positive-ion ESI-MS ion cluster at m/z 2892 $\{M + H^+ - 2 \times PF_6^-\}^{3+}$, 2844 $\{M - 3 \times PF_6^-\}^{3+}$, 2242 $\{M + 4 \times H^+\}^{4+}$, 2207 $\{M + 3 \times H^+ - PF_6^-\}^{4+}$, 2171 $\{M + 2 \times H^+ - 2 \times PF_6^-\}^{4+}$, 2133 $\{M + H^+ - 3 \times PF_6^-\}^{4+}$, 2097 $\{M - 4 \times PF_6^-\}^{4+}$, 1766 $\{M + 4 \times H^+ - PF_6^-\}^{5+}$, 1735 $\{M + 3 \times H^+ - 2 \times PF_6^-\}^{5+}$, 1707 $\{M + 2 \times H^+ - 3 \times PF_6^-\}^{5+}$, 1677 $\{M + H^+ - 4 \times PF_6^-\}^{5+}$, 1649 $\{M - 5 \times PF_6^-\}^{5+}$. IR (KBr) ν/cm^{-1}: 3424 (s, br, N−H), 1657 (s, C═O), 847 (s, PF_6^-). Anal. Calcd for $Ir_8C_{398}H_{352}N_{58}O_{20}P_8F_{48}\cdot 6H_2O$: C, 53.87; H, 4.41; N, 8.63. Found: C, 54.09; H, 4.66; N, 8.80.

[{Ir(pq)$_2$}$_4$(bpy-4)](PF$_6$)$_4$ (pq-4). The procedure was similar to that for the preparation of complex **ppy-4**, except that [Ir$_2$(pq)$_4$Cl$_2$] was used instead of [Ir$_2$(ppy)$_4$Cl$_2$]. Subsequent recrystallization from CH_2Cl_2/diethyl ether afforded complex **pq-4** as orange crystals. Yield: 40%. ^{1}H NMR (300 MHz, $(CD_3)_2CO$, 298 K, TMS): δ 8.65 (br, 4H, CONH), 8.54−8.41 (m, 20H, H3 of bpy and H3 of phenyl ring and H3 of quinoline of pq), 8.31−8.17 (m, 20H, H3′, H6, and H6′ of bpy and H4 of quinoline of pq), 7.96 (d, 4H, J = 6.0 Hz, H5 of bpy), 7.86−7.82 (m, 8H, H8 of quinoline of pq), 7.62 (br, 4H, CONH), 7.54 (d, 4H, J = 5.4 Hz, H5′ of bpy), 7.42−7.31 (m, 16H, H5 and H7 of quinoline of pq), 7.19−7.05 (m, 16H, H4 of phenyl ring and H6 of quinoline of pq), 6.84−6.74 (m, 8H, H5 of phenyl ring of pq), 6.54−6.49 (m, 8H, H6 of phenyl ring of pq), 3.47−3.26 (m, 16H, CONHCH_2 and CH_2NHCO), 3.07 (br, 8H, NCH_2), 2.58−2.46 (m, 12H, CH_2N and CH_2CO), 2.39 (s, 12H, CH_3 on C4′ of bpy). Positive-ion ESI-MS ion cluster at m/z 2070 $\{M + H^+ - PF_6^-\}^{2+}$, 1998 $\{M - 2 \times PF_6^-\}^{2+}$, 1331 $\{M + H^+ - 2 \times PF_6^-\}^{3+}$, 1283 $\{M - 3 \times PF_6^-\}^{3+}$. IR (KBr) ν/cm^{-1}: 3422 (s, br, N−H), 1660 (s, C═O), 847 (s, PF_6^-). Anal. Calcd for $Ir_4C_{190}H_{160}N_{26}O_8P_4F_{24}\cdot 4CH_2Cl_2$: C, 50.39; H, 3.66; N, 7.88. Found: C, 50.18; H, 3.74; N, 8.08.

[{Ir(pq)$_2$}$_3$(bpy-3)](PF$_6$)$_3$ (pq-3). The procedure was similar to that for the preparation of complex **ppy-3**, except that [Ir$_2$(pq)$_4$Cl$_2$] was used instead of [Ir$_2$(ppy)$_4$Cl$_2$]. Subsequent recrystallization from CH_2Cl_2/diethyl ether afforded complex **pq-3** as orange crystals. Yield: 42%. ^{1}H NMR (300 MHz, $(CD_3)_2CO$, 298 K, TMS): δ 8.67 (br, 3H, CONH), 8.55−8.36 (m, 15H, H3 of bpy and H3 of phenyl ring and H3 of quinoline of pq), 8.26−8.16 (m, 15H, H3′, H5, and H6 of bpy and H4 of quinoline of pq), 7.90−7.83 (m, 9H, H6′ of bpy and H8 of quinoline of pq), 7.55 (d, 3H, J = 4.8 Hz, H5′ of bpy), 7.40−7.24 (m, 12H, H5 and H7 of quinoline of pq), 7.20−7.09 (m, 6H, H4 of phenyl ring of pq), 7.06−6.91 (m, 6H, H6 of quinoline of pq), 6.85−6.73 (m, 6H, H5 of phenyl ring of pq), 6.56−6.50 (m, 6H, H6 of phenyl ring of pq), 3.36 (br, 6H, CONHCH_2), 2.68 (br, 6H, NCH_2), 2.30 (s, 9H, CH_3 on C4′ of bpy). Positive-ion ESI-MS ion cluster at m/z 2827 $\{M - PF_6^-\}^+$, 1341 $\{M - 2 \times PF_6^-\}^{2+}$. IR (KBr) ν/cm^{-1}: 3421 (s, br, N−H), 1666 (s, C═O), 846 (s, PF_6^-). Anal. Calcd for $Ir_3C_{132}H_{102}N_{16}O_3P_3F_{18}\cdot 2H_2O$: C, 52.71; H, 3.55; N, 7.45. Found: C, 52.57; H, 3.64; N, 7.50.

Physical Measurements and Instrumentation. Equipment for the characterization, photophysical, electrochemical, lipophilicity,

and cytotoxicity measurements, has been described previously.[43i] Luminescence quantum yields were measured by the optically dilute method[58] using an aerated aqueous solution of $[Ru(bpy)_3]Cl_2$ ($\Phi = 0.028$) as the standard solution.[59] The lipophilicity and cytotoxicity have been determined with the reported methods.[43i]

Agarose Gel Retardation Assays. Agarose gel retardation assays were used to study the DNA condensation ability of the complexes. Plasmid DNA (1 μg) was mixed with the iridium(III) complex with [Ir] ranging from 12.5 to 400 nM in PBS/DMSO (10 μL, 7:3, v/v). The mixture was incubated at room temperature for 30 min and then electrophoresced (Power-Pac, Bio-Rad, 100 V, 40 min) on a 0.9% (w/v) agarose gel containing ethidium bromide (0.5 μg/mL) in Tris-acetate-EDTA (TAE) buffer. The agarose gel was examined by the Bio-Rad Gel Doc imager.

ICP-MS. HeLa cells were grown in a 60 mm tissue culture dish and incubated at 37 °C under a 5% CO_2 atmosphere for 48 h. The culture medium was removed and replaced with medium/DMSO (99:1, v/v) containing the complex at [Ir] = 2 μM. After incubation for 3 h, the medium was removed, and the cell layer was washed gently with PBS (1 mL × 3). After that, the cell layer was trypsinized, digested in 65% HNO_3 (2 mL) at 70 °C for 2 h, and then diluted in Milli-Q water to the final volume of 10 mL for ICP-MS (PerkinElmer SCIEX, ELAN DRC Plus) analysis.

Confocal Microscopy. HeLa cells were grown on a sterile glass coverslip in a 35 mm tissue culture dish. The incubation procedure was similar to that of the ICP-MS. After washing with PBS, the coverslip was mounted onto slides for measurements. Imaging was performed using a confocal microscope (Leica TCS SPE) with an excitation wavelength at 405 nm. The emission was measured using a long-pass filter at 532 nm. In the 4 °C imaging experiments, HeLa cells were preincubated at 4 °C for 1 h before treatment with complexes. In the co-staining experiments, after treated with complexes, the HeLa cells were fixed by PBS containing 3% paraformaldehyde, and then incubated with anti-golgin-97 (human) mouse IgG_1 (1 μg/mL, 1 h), washed with PBS (1 mL × 3), then incubated with Alexa 635 goat anti-mouse IgG (H+L) (10 μg/mL, 30 min), and finally washed with PBS (1 mL × 3).

Flow Cytometry. The incubation procedure was similar to that for the ICP-MS measurements. After washing with PBS, the cell layer was trypsinized and added up to a final volume of 2 mL with PBS. The samples were analyzed by a FACSCalibur flow cytometer (Becton, Dickinson and Co., Franklin Lakes, NJ, U.S.A.) with excitation at 488 nm. The emission was measured using a long-pass filter at 505 nm. The number of cells analyzed for each sample was between 9,000 and 10,000.

Acknowledgment. We thank The Hong Kong Research Grants Council (Project Nos. CityU 101606 and 101908) for financial support. K.Y.Z. acknowledges the receipt of a Postgraduate Studentship, a Research Tuition Scholarship, and an Outstanding Academic Performance Award, all of which were administered by the City University of Hong Kong.

Supporting Information Available: Laser-scanning confocal microscopy images (*z* stacks) of HeLa cells incubated with complex **pq-1**. This material is available free of charge via the Internet at http://pubs.acs.org.

(58) Demas, J. N.; Crosby, G. A. *J. Phys. Chem.* **1971**, *75*, 991–1024.
(59) Nakamura, K. *Bull. Chem. Soc. Jpn.* **1982**, *55*, 2697–2705.